MIJST
MIST International Journal of Science and Technology

Bit Error Rate Performance in CDMA Free Space Optical Links with SIK Receiver under Fog Conditions

A. K. M. Nazrul Islam[1*] and S. P. Majumder[2]

[1]Department of Electrical Electronic and Communication Engineering, Military Institute of Science and Technology, Bangladesh
[2]Department of Electrical and Electronic Engineering, Bangladesh University of Engineering and Technology, Bangladesh

emails: *[*1]nazrul_4620@yahoo.com and [2]spmajumder@eee.buet.ac.bd*

ARTICLE INFO

Article History:

Received: 14th February 2023
Revised: 26th August 2023
Accepted: 27th August 2023
Published: 28th December 2023

Keywords:

OCDMA
Double gamma function
BER
Multiple Access Interference (MAI)
Sequence Inverse Keying (SIK)

ABSTRACT

This article presents a novel analytical method for evaluating fog's impact on Bit Error Rate (BER) in an Optical Code Division Multiple Access (OCDMA) Free Space Optical (FSO) connection. The investigation employs an optical encoder and direct detection receiver employing a balanced photo detector with Sequence Inverse Keying (SIK) to explore fog effects. By scrutinizing multi-access interference (MAI) current and signal current values at the SIK receiver's output under varied fog conditions, we deduce BER expressions for diverse scenarios. These encompass different fog thickness levels, code lengths, simultaneous users, and system parameters. The results reveal substantial OCDMA degradation due to fog thickness and users. Also, the system incurs a marked power penalty at a specific BER, especially with higher fog and user density. However, we identify a potential solution: increasing code length, effectively mitigating fog-induced performance decline.

1. INTRODUCTION

Being an attractive and economical choice, the Free-Space Optical (FSO) communication presents a substitute for conventional Optical Fiber Communication (OFC), particularly in situations where deploying fiber optic infrastructure is economically and logistically challenging (Singh *et al.*, 2021). However, the effectiveness of FSO techniques can be compromised by various weather-centric elements, such as turbulence, pointing inaccuracies, haze, fog, clouds, rain, and snow, leading to performance degradation (Mahalati, 2012; Yang, 2014; Esmail *et al.*, 2019; Sunilkumar *et al.*, 2019; Ashrafzadeh *et al.*, 2020). Accurately comprehending the influence of these atmospheric conditions on the propagation of optical signals through the atmosphere remains a significant quandary for the research community. Consequently, numerous scholarly endeavors have been undertaken to model the repercussions of rain, cloud, fog, and haze on FSO communication systems (Grabner, 2014; Mori, 2015; Kalesnikau *et al.*, 2021; Yasir *et al.*, 2022; Al-Gailani *et al.*, 2021).

To characterize the temporal dynamics of optical pulses as they traverse through fogs, mathematical models rooted in the double gamma function have been formulated through the utilization of Monte Carlo simulation methods (Aharonovich *et al.*, 2005). Furthermore, explorations into the wavelength-dependent behavior of the extinction coefficient and attenuation across rain, fog, snow, and haze have been executed (Grabner, 2014).

In contrast, optical code division multiple access (OCDMA) has amassed substantial attention for its applicability in optical fiber networks, providing multiple users with access to the network through distinct orthogonal codes. Significant scholarly inquiry into OCDMA-based fiber optic communication systems has been undertaken over the past decade to evaluate capacity and impairments linked to fiber-based communication approaches (Majumder *et al.*, 2005). Furthermore, the efficacy of OCDMA systems over FSO channels under the influence of atmospheric turbulence has been systematically explored both analytically and computationally (Bai, 2015; Liu, 2011). Notably, recent attention has been directed toward FSO communication via fog and clouds, employing ultra-short laser filaments of considerable intensity, with efforts to understand its feasibility (Schimmel *et al.*, 2018).

In this study, we introduce an innovative analytical technique aimed at assessing the performance of Bit Error Rate (BER) in a Free-Space Optical Code Division Multiple Access (FSO OCDMA) system. Our methodology involves the utilization of an OCDMA encoder combined with a receiver based on Sequence

Inverse Keying (SIK). This approach builds upon the foundational work previously established by researchers such as Majumder (2005) and O'Farrell (1995). The primary objective of our investigation is to gain a comprehensive understanding of how three critical parameters – namely, fog thickness, code length of the OCDMA encoder, and the count of concurrent users – collectively influence the overall system performance.

To achieve this objective, we conduct an extensive array of numerical assessments across varying conditions, encompassing different code lengths of the OCDMA encoder, diverse counts of simultaneous users, and varying fog thickness levels. By simulating various scenarios, we acquire invaluable insights into the system's behavior within practical, real-world settings. Furthermore, we quantify the power penalty incurred due to the interplay of fog and the simultaneous user count, thereby optimizing system performance to meet specific BER targets. The primary contributions of our research are outlined as follows:

- Introduction of a novel analytical framework for evaluating BER performance within the context of FSO OCDMA systems.
- Investigation of the impacts of fog thickness, OCDMA encoder code length, and count of simultaneous users on the system's performance.
- Extensive numerical analysis of the system's behavior across a range of different scenarios.
- Quantification of the power penalty attributed to the combined effects of fog and the number of simultaneous users, tailored to meet precise BER requirements.

2. MODELLING OF FSO SYSTEM

The central challenge in the deployment of OCDMA network and communication pertains to the formulation of encoding and decoding approaches essential for the generation and identification of suitable code sequences. The configuration of a transmitter and a direct-detection receiver for the OCDMA system is depicted in Figure 1.

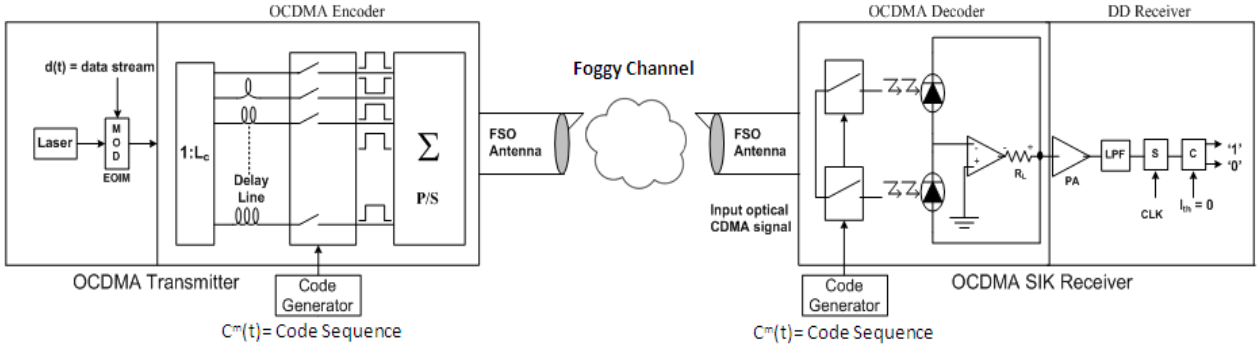

Figure 1: An optical CDMA (OCDMA) setup featuring an SIK dual photodetector direct detector receiver, operating across a fog impacted Free-Space Optical (FSO) communication channel

In accordance with the binary values '1' or '0', the transmitter modulates the user's data using either a unipolar signature sequence or its constituent elements. Within this framework, an optically switched correlator receiver is employed, operating on the underlying principle of unipolar-bipolar correlation. Specifically, the bipolar reference sequence is subjected to direct correlation with the unipolar reference sequence of the channel, facilitating the retrieval of users' data.

3. FOG TRANSFER FUNCTION

The double gamma function, as introduced by Aharonovich *et al.* in 2005, serves as a widely acknowledged model suitable for characterizing the temporal impulse response inherent to an optical wireless channel in foggy conditions. The functional representation of this model takes the form:

$$h_f(t) = [k_1 t\ exp(-k_2 t) + k_3 t\ exp(-k_4 t)]P_o u(t) \quad (1)$$

In this equation, the parameters k_i correspond to factors extracted from empirical gamma function analysis, $u(t)$ denotes the unit step function, and P_o represents the cumulative impact of power loss attributed to phenomena like scintillation effects, beam divergence, and optical imperfections. By performing a Fourier transformation on equation (1), the transfer function of the optical wireless channel can be evaluated as demonstrated in the work by Aharonovich *et al.* in 2005:

$$H_f(\omega) = \int_0^\infty h_f(t)\, exp(-j\omega t)dt \quad (2)$$

Substituting (1) in (2) and integrating we get:

$$H_f(\omega) = \left[\frac{k_1}{(k_2 - j\omega)^2} + \frac{k_3}{(k_4 - j\omega)^2}\right] P_o \quad (3)$$

The following function is thus used to estimate the channel power loss:

$$H_f(0) = \left(\frac{k_1}{k_2^2} + \frac{k_3}{k_4^2}\right) P_o \quad (4)$$

An optical wireless channel's temporal dispersion is determined by (1), which is referred to as the channel's *rms* delay dispersion D.

$$D = \left[\frac{\int_{-\infty}^{\infty}(t-\mu)^2 h_f^2(t)dt}{\int_{-\infty}^{\infty} h_f^2(t)dt}\right]^{\frac{1}{2}} \quad (5)$$

The mean delay μ is defined by:

$$\mu = \left[\frac{\int_{-\infty}^{\infty} th^2(t)dt}{\int_{-\infty}^{\infty} h^2(t)dt}\right] \quad (6)$$

The mean delay μ and rms delay spread D can be calculated using equations (7) and (8), employing the expressions (1) provided in equations (5) and (6). Equation (7) gives the mean delay μ as follows:

$$\mu = \frac{3\left[\frac{k_1^2}{k_2^4}+\frac{k_3^2}{k_4^4}+\frac{32k_1k_3}{(k_2+k_4)^4}\right]}{2\left[\frac{k_1^2}{k_2^3}+\frac{k_3^2}{k_4^3}+\frac{16k_1k_3}{(k_2+k_4)^3}\right]} \quad (7)$$

$$D = \left\{\begin{array}{c}\left[\frac{k_1^2}{k_2^3}+\frac{k_3^2}{k_4^3}+\frac{16k_1k_3}{(k_2+k_4)^3}\right]\times \\ \left(\begin{array}{c}\frac{k_1^2[3+\mu k_2(\mu k_2-3)]}{k_2^5}+\frac{k_3^2[3+\mu k_4(\mu k_4-3)]}{k_4^5}+ \\ \frac{16k_1k_3\{12+\mu(k_2+k_4)[\mu(k_2+k_4)-6]\}}{(k_2+k_4)^5}\end{array}\right)\end{array}\right. \quad (8)$$

The normalized delay spread, denoted as DT, is calculated by taking the quotient of the root mean square (rms) delay spread and the duration of a single bit.

4. ANALYSIS OF THE SYSTEM

The OCDMA signal linked with the transmission of the m^{th} user can be formulated as shown below:

$$S_m(t) = 2P_T.\sum_{k=0}^{\infty} a_k^m g(t-kT_b) \times C^m(t)e^{j\omega_c t} \quad (9)$$

In this equation, P_T represents the average transmitted power, a_k^m signifies the *k*th bit of the *m*th user, *g*(*t*) describes the pulse shape of the data bit, T_b denotes the duration of a bit, and ω_c stands for the angular frequency of the optical carrier.

The code utilized by the m^{th} user is defined as follows:

$$C^m(t) = \sum_{l=o}^{Lc-1} C_l^m p(t-lT_c) \quad (10)$$

Within Equation (10), C_l^m symbolizes the l^{th} chip of the m^{th} user codeword, T_c denotes the chip period (T_c=T_b/L_c), L_c corresponds to the code length, often referred to as processing gain, *Gp*, and *p(t)* represents the pulse shape of the individual chip.

Utilizing Equation (10) in (9), $S_m(t)$ can be derived as follows:

$$S_m(t) = \begin{cases}2P_T.\sum_{k=0}^{\infty} a_k^m.g(t-kT_b)\times \\ \sum_{l=1}^{L_c} C_l^m p(t-lT_c).e^{j\omega_c t}\end{cases} \quad (11)$$

Equations (9) through (11) are employed for the subsequent analysis in order to assess the BER expression. The optical response corresponding to the m^{th} user at the fog's output, distinguished by the impulse response $h_f(t)$ can be expressed as follows:

$$Y_{mf}(t) = \begin{cases}2P_T.\sum_{k=0}^{\infty} a_k^m g(t-kT_b)\times \\ \sum_{l=1}^{L_c} C_l^m\left[p(t-lT_c)\otimes h_f(t)\right].e^{j\omega_c t}\end{cases} \quad (12)$$

The formulation in Equation (12) can be restated as follows, where $p_f(t) = p(t) \otimes h_f(t)$ indicating the form of the chip configuration at the fog's reception terminus.

$$Y_{mf}(t) = \begin{cases}2P_T.\sum_{k=0}^{\infty} a_k^m g(t-kT_b)\times \\ \sum_{l=1}^{L_c} C_l^m p_f(t-lT_c).e^{j\omega_c t}\end{cases} \quad (13)$$

The resultant optical signal in the presence of fog can then be described as:

$$r_o(t) = \begin{cases}\sum_{m=1}^{M} 2P_r.\sum_{k=0}^{\infty} a_k^m g(t-kT_b)\times \\ \left\{\sum_{l=1}^{L_c} C_l^m p_f(t-lT_c)\right\}e^{j\omega_c t}+n_b(t)\end{cases} \quad (14)$$

In this equation, $n_b(t)$ denotes the additive white noise. On account of a SIK correlator receiver (O'Farrell, 1995; Majumder, 2005), for each user indexed by *i*, the receiver's output current can be derived as follows:

$$Z_i(t) = \begin{cases}\frac{R_d P_r}{2}\int_0^{T_b}\sum_{m=1}^{M} a_k^m g(t-kT_b)\times \\ \sum_{l=1}^{L_c} C_l^m p_f(t-lT_c)\times \\ \left\{C^i(t-lT_c)-\overline{C^i(t-lT_c)}\right\}dt+i_n(t)\end{cases} \quad (15)$$

Here, $i_n(t)$ denotes the noise current associated with the photodetector and the receiver, and R_d represents the responsivity.

The average photocurrent $Z_i(t)$ is thus defined as:

$$U = \frac{R_d P_r}{4T_b}\int_0^{T_b}\sum_{l=1}^{L_c-1} p_f(t-lT_c)dt \quad (16)$$

The statistical dispersion of Multiple Access Interference (MAI) as reported in prior works [9, 10]:

$$\sigma_{MAI}^2 = U^2.\frac{2(M-1)}{3L_c} \quad (17)$$

Thus, we can compute statistical dispersion of $i_n(t)$ as follows:

$$\sigma_n^2 = \sigma_{th}^2 + \sigma_{shot}^2 = \frac{4K_bTB}{R_L} + 2eB\left(I_{sig}+I_b\right) \quad (18)$$

This equation consequently redefines the Signal-to-Noise plus Interference Ratio (SNIR) as follows:

$$\xi = \frac{U^2}{\sigma_n^2+\sigma_{MAI}^2} \quad (19)$$

The ultimate BER is thus can be determined using the well-known relation (Yang *et al.* 2014):

$$BER = \frac{1}{2}erfc\left[\frac{\sqrt{\xi}}{2\sqrt{2}}\right] \quad (20)$$

This equation allows for the estimation of BER, indicating the considered wireless communication system's performance limits under foggy conditions.

5. EXPERIMENTAL RESULTS AND ANALYSIS

Utilizing the analytical methodology outlined in Section 4, we proceed to assess performance in terms of BER for an OCDMA FSO system with SIK under foggy conditions. This evaluation involves varying system parameters, as detailed in Table 1, and employs double Gamma function constants to account for fog thickness ranging from 200 m to 300 m.

Table 1
Parameters of the System

Parameter	Symbol	Value
Data transmission rate	R_b	10 Mbps
Responsiveness	R_d	0.85 A/W
Bandwidth of the receiver	B	1 MHz
Receiver load impedence	R_L	50 Ω
Temperature at receiver	T	300^0 K
Current due to noise	I_b	10 nA
Elementary charge	e	1.602x10^{-19} C
Boltzmann's constant	K_b	1.38x10^{-23} W/K/Hz
Fog density within medium	-	200-300 m
Users quantity	M	1 - 128
Operational wavelength	λ	0.532 µm
Length of coding sequence	$L_c(Gp)$	8 - 1024
Power penalty at BER	-	10^{-9}

Figures 2 and 3 depict BER trends against received optical power (Io in dBm) for distinct scenarios: in Figure 2, the system deploys a code length of 256 and accommodates 8 users, while Figure 3 considers a code length of 1024 and 16 users, all operating at a bit rate of 10 Mbps. These figures highlight a noticeable escalation in BER with increasing fog thickness, signifying the significant influence of fog within the channel.

Furthermore, Figure 2 reveals the emergence of a BER floor due to the interplay of MAI, fog-induced effects, and optical channel characteristics. The reduction of this flooring effect can be significantly addressed by employing higher processing gain, as highlighted in Figure 4. The significant improvement in BER performance is evident from both Figure 2 and Figure 3 when the processing gain (G_p) is elevated from 256 to 1024. This improvement remains consistent even as the count of concurrent users rises from 8 to 16.

Figure 4 delves into the impact of code length (Gp) on BER, accounting for a fog thickness of 250 m and 16 simultaneous users at 10 Mbps data transmission rate. Here, a positive correlation is observed between higher code lengths and improved BER performance, while reduced processing gain adversely affects the system's performance.

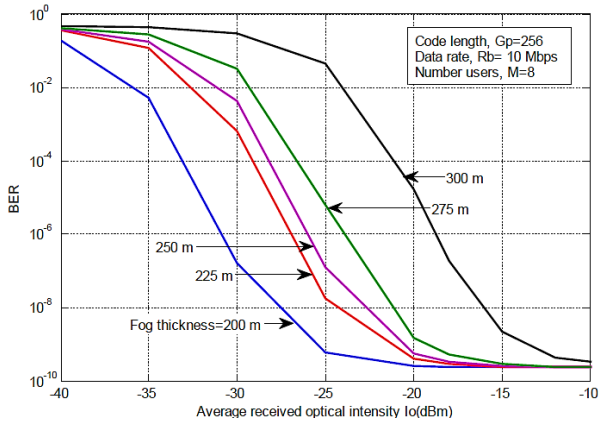

Figure 2: Plotting BER against the average optical intensity at the receiver (Io in dBm) is shown for a code length of 256 (Gp=256) and 8 users (M=8). The data rate is set at 10 Mbps (Rb=10 Mbps), and the investigation involves changing the thickness of fog

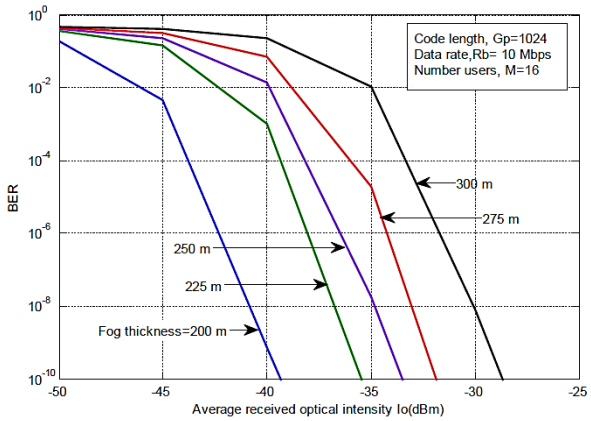

Figure 3: Plotting BER against the average optical intensity at the receiver, Io(dBm), is depicted for a code length of Gp=1024 and M=16 users. The data rate is Rb=10 Mbps, and the investigation involves altering the thickness of the fog layer

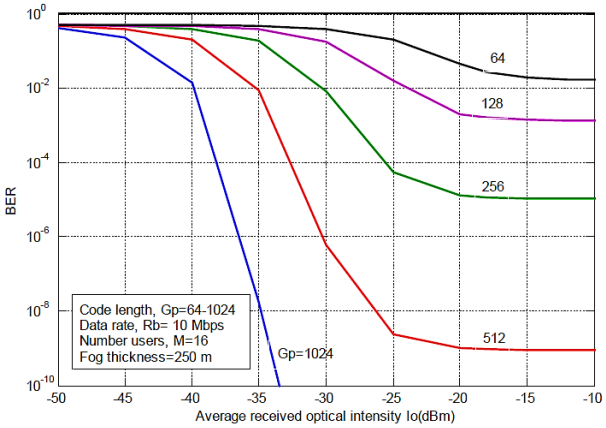

Figure 4: Plotting BER against the average optical intensity at the receiver, Io(dBm), in the presence of fog with a thickness of 250 m. The system includes 16 users (M=16) at a data rate of 10 Mbps (Rb=10 Mbps), with adjustments made to the code length Gp

The BER trends against the intensity (I_o in dBm) of optical signal at the receiver are outlined in Figure 5. This analysis, conducted at a constant length of a code sequence, i.e., Gp =512 and retaining 300 m fog thickness, underscores the BER's rise with an augmented number of simultaneous users. Remarkably, this trend continues unabated beyond 16 users, with BER floors manifesting. Similar behavior is detected in the BER trends under the effect of varying fog thicknesses.

To elucidate the relationship between the count of simultaneous users and power penalty, Figure 6 presents the power penalty plots. In particular, the scenario being examined involves keeping the value of code length (Gp) 1024, the data rate (Rb) of 10 Mbps, and retaining the BER in the range of 10^{-9} consistently. Notably, an almost linear increase in power penalty is evident as the number of simultaneous users escalates, holding fog optical thickness as a variable.

The interdependence between fog thickness and power penalty is observed in Figure 6. For instance, the penalty incurred by the 15th user at a fog thickness of 200 m surpasses 3 dB, escalating to 14dB having a 300 m fog

thickness. In other words, the penalty exhibits variations at intermediate fog thicknesses, such as 7.5 dB, 9.5 dB, and 11.25 dB for fog thicknesses of 225 m, 250 m, and 275 m, respectively.

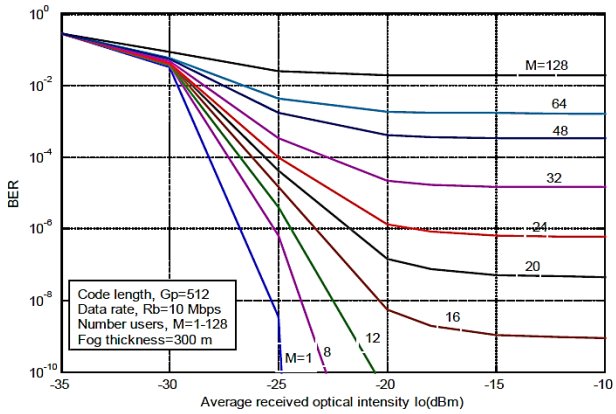

Figure 5: Plotting of BER against the average optical intensity at the receiver, Io(dBm), for a code length of Gp=512 and fog depth of 300 m. The data rate is set at Rb=10 Mbps, with adjustments made to the user count M

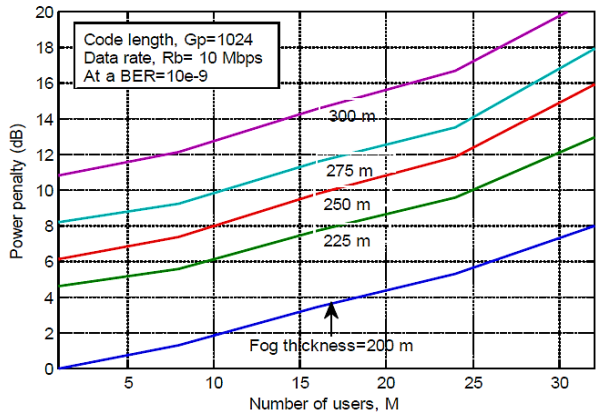

Figure 6: Change in power penalty as a function of the number of users (M) for a code length of 1024, data rate of 10 Mbps, and variable fog thickness, with a bit error rate (BER) of 10 to the power of -9

6. CONCLUSIONS

In this research, we introduced a new approach to analytically evaluate the fog impact on an OCDMA FSO link with an SIK receiver. Our findings underscore that increasing fog thickness and simultaneous users lead to significant power penalty and BER degradation, factoring in channel effects. However, we identified that adopting longer code lengths and minimizing fog thickness effectively mitigates the power penalty.

This study holds pivotal importance for designing OCDMA systems in FSO links, addressing atmospheric turbulence, pointing errors, and fog-related challenges. By providing actionable solutions, it enhances system performance in adverse weather. Beyond its technical contributions, our work illuminates a path for advancing optical communication networks and stimulating further related research.

Our approach stands as a cornerstone in building robust FSO links, enabling dependable communication amidst harsh weather conditions. This transformative potential not only extends the boundaries of research but also propels practical applications, marking a new era in resilient optical communication.

ACKNOWLEDGEMENTS

This research was conducted as a part of a Ph.D. dissertation in the EEE Department at BUET, Dhaka, Bangladesh.

REFERENCES

Aharonovich, M. & Arnon, S. (2005). Performance improvement of optical wireless communication through fog with a decision feedback equalizer. Journal of Optical Society of America A, 22(8), 1646-1654. DOI: 10.1364/JOSAA.22.001646

Ali, M. (2012). Free Space Lasers Propagation at Different Weather Conditions. Al- Mustansiriyah Journal Science, 23(2), 81-90

Ashrafzadeh, B., Zaimbashi, A., Soleimani-Nasab, E., & Uysal, M. (2020). Unified Performance Analysis of Multi-Hop FSO Systems Over Double Generalized Gamma Turbulence Channels with Pointing Errors. IEEE Transactions on Wireless Communications, 19(11), 7732–7746. https://doi.org/10.1109/twc.2020.3015780

Al-Gailani, S. A., Mohd Salleh, M. F., Salem, A. A., Shaddad, R. Q., Sheikh, U. U., Algeelani, N. A., & Almohamad, T. A. (2021). A Survey of Free Space Optics (FSO) Communication Systems, Links, and Networks. IEEE Access, 9, 7353–7373. https://doi.org/10.1109/access.2020.3048049

Bai, F., Su, Y. & Sato, T. (2015). Performance Analysis of Heterodyne-Detected OCDMA Systems Using PoISK Modulation over a Free-Space Optical Turbulece Channel. Photonics, 4(4), 785-798. DOI: https://doi.org/10.3390/electronics4040785

Esmail, M. A., Ragheb, A. M., Fathallah, H. A., Altamimi, M., & Alshebeili, S. A. (2019). 5G-28 GHz Signal Transmission Over Hybrid All-Optical FSO/RF Link in Dusty Weather Conditions. IEEE Access, 7, 24404–24410. https://doi.org/10.1109/access.2019.2900000

Grabner, M. & Kvicera, V. (2014). Multiple scattering in Rain and Fog on Free-Space Optical Links. Journal of Lightwave Technology, 32(3), 513-519.

Kalesnikau, I., Pioro, M., Rak, J., Ivanov, H., Fitzgerald, E., & Leitgeb, E. (2021). Enhancing Resilience of FSO Networks to Adverse Weather Conditions. IEEE Access, 9, 123541–123565. https://doi.org/10.1109/access.2021.3107243

Liu, P., Wu, X., Wakamori, K., et. al. (2011). Bit Error Rate Performance Analysis of Optical CDMA Time Diversity Links over Gamma-Gamma Atmospheric Turbulence Channel. IEEE Conference on Wireless Communications and Networking (WCNC), 1932-1936. DOI: https://doi.org/10.1109/WCNC.2011.5779454

Mahalati, R, N. & Kahn, J, M. (2012). Effect of fog on free-space optical links employing imaging receivers. Optics Express, 20(2), 1649-1661. DOI: https://doi.org/10.1364/OE.20.001649

Majumder, S, P., Azhari, A. & Abbou, F, M. (2005). Impact of Fiber Chromatic Dispersion on the BER Performance of an Optical CDMA IM/DD Transmission System. IEEE Photonic Technology Letters, 17(6), 1340-1342. DOI: 10.1109/LPT.2005.846924

Mori, S., & Marzano, F, S. (2015). Microphysical characterization of free space optical link due to hydrometeor and fog effects. Applied Optics, 54(22), 6787-6803. DOI: 10.1364/AO.54.006787

Nebuloni, R. & Capsoni, C. (2014). Sensitivity of laser attenuation through fog to the wavelength and to the drop size distribution. 19th European Conference on Networks and Optical Communications - (NOC), 86-90. DOI: 10.1109/NOC.2014.6996833

O'Farrell, T. & Lochmann, S, I. (1995). Switched correlated receiver architecture for optical CDMA networks with bipolar capacity. Electronic Letters, 31(11), 905-906.

Schimmel, G., Proudit, T., Morgin, D., Kasparin, J., & Wolf, J, P. (2018). Free Space Laser Telecommunication through Fog. Optica, 5(10), 1338-1341. DOI: https://doi.org/10.1364/OPTICA.5.001338

Singh, H., Mittal, N., Miglani, R., Singh, H., Gaba, G. S., & Hedabou, M. (2021, October). Design and Analysis of High-Speed Free Space Optical (FSO) Communication System for Supporting Fifth Generation (5G) Data Services in Diverse Geographical Locations of India. IEEE Photonics Journal, 13(5), 1–12. https://doi.org/10.1109/jphot.2021.3113650

Sunilkumar, K., Anand, N., Satheesh, S. K., Krishna Moorthy, K., & Ilavazhagan, G. (2019, April 9). Performance of free-space optical communication systems: effect of aerosol-induced lower atmospheric warming. Optics Express, 27(8), 11303. https://doi.org/10.1364/oe.27.011303

Yasir, S. M., Abas, N., Rauf, S., Saleem, M. S., & Haider, A. (2022). Performance Analysis of Dual-Beam Free Space Optical Communication Link under Dust and Rain Conditions. Wireless Communications and Mobile Computing, 2022, 1–15. https://doi.org/10.1155/2022/9060676

Yang, F., Cheng, J. & Tsiftsis, T. (2014). Free-space optical communication with nonzero boresight pointing errors. IEEE Transactions on Communication, 62(2), 713-725. DOI: 10.1109/TCOMM.2014.010914.130249